Transcriptional Analysis of Multisite Drug–DNA Dissociation Kinetics: Delayed Termination of Transcription by Actinomycin D†

Robin J. White and Don R. Phillips*
Department of Biochemistry, La Trobe University, Bundoora, Victoria 3083, Australia
Received April 1, 1988; Revised Manuscript Received July 6, 1988

ABSTRACT: An in vitro transcription assay was used to measure the relative occupancy, sequence specificity, and dissociation kinetics of six actinomycin D binding sites on DNA during conditions of active transcription of the DNA from the *lac* UV5 promoter. Five of the sites contained a GpC sequence, with three of these having a common AGCT sequence that differed by up to an order of magnitude in affinity for the drug, as indicated by their relative occupany and dissociation kinetics. Positive cooperativity was observed by higher occupancy and slower dissociation kinetics for neighboring GpC sites on a different DNA fragment (UV5-λP_L). Termination of transcription was observed at some drug binding sites, while complete drug-induced termination of transcription was seen 7–10 nucleotides downstream of two drug sites. This delayed termination was minimized when ITP was incorporated into the transcripts and suggests that a time delay is required to enable stable RNA hairpin helices to form. A model is presented of the role of RNA hairpin helices in delayed, drug-induced termination of transcription. The classical picture of DNA-binding drugs as inhibitors of transcription now appears too simplistic as it does not accommodate this phenomenon. It will be important to gain a greater understanding of the mechanism of this phenomenon of drug-induced termination of transcription, as there are many implications for the design of DNA-acting drugs.

Anticancer drugs presently in use, and many of those in clinical trials, are believed to exert their activity by binding to DNA (Wilson & Jones, 1981; Neidle & Waring, 1983). With these drugs, a long-standing question has been whether this effect is due to the thermodynamic affinity of the drug for DNA or the kinetics of dissociation of drug from the DNA and has not yet been resolved (Brown, 1978; Wilson & Jones, 1981; Siegfried et al., 1983; Ralph et al., 1983). There is good evidence to support the notion of affinity being the dominant factor, as illustrated by the correlation of DNA binding affinity with biological activity for a series of anthracycline derivatives spanning 3 orders of magnitude of both parameters (Valentini et al., 1985). There is also an increasing amount of evidence in support of the concept that the dissociation kinetics are an important determinant of anticancer activity (Gabbay et al., 1976; Wilson et al., 1976; Aktipis & Panayotatos, 1981; Wakelin & Waring, 1980; Fox & Waring, 1981; Waring & Fox, 1983; Feigon et al., 1984; Denny et al., 1985; Gandecha et al., 1985; Wakelin et al., 1987).

If the drug–DNA dissociation kinetics are indeed an important aspect of biological activity of the drug, it becomes critical to establish which biological or physicochemical procedures yield meaningful values for the dissociation process. The most rigorous physicochemical procedures for analysis of drug–DNA kinetics involve *T*-jump or stopped-flow relaxation methods (Bernasconi, 1976; Chaires et al., 1985) but are exceedingly laborious, tedious, and time-consuming. A more rapid procedure that yields just the dissociation kinetic parameters is a detergent sequestering technique pioneered by Muller and Crothers (1968) and widely employed since then for a variety of DNA-binding drugs (Chaires et al., 1985; Wakelin, 1986). While this technique provides an extremely rapid means of quantitating drug–DNA dissociation kinetics, they are complicated by the contribution to the kinetic parameters of the foward reaction(s) and by the possible effects of the detergent on the stability of the drug–DNA complex.

A new procedure has recently been established to yield drug–DNA dissociation kinetics under conditions of active transcription of the DNA (Phillips & Crothers, 1986). This procedure yields a physiologically more meaningful measure of dissociation kinetics than the physicochemical procedures outlined above. A surprising result obtained from this transcription assay was that the time constant for dissociation of drug from the DNA (i.e., residence time) was longer as measured by the transcription assay than by detergent sequestration (Phillips & Crothers, 1986). This was unexpected since transcription involves opening of the DNA adjacent to the drug binding site, with a presumed concomitant destabilization of the drug–DNA complex. The most likely explanation for these observations is that in the detergent sequestering procedure an average value is measured, reflecting dissociation from a range of drug binding sites. This averaged value must be compared with that detected by the transcription assay, where dissociation from a single defined site is measured. The implication of this interpretation is that the range of dissociation time constants would also be detected by the transcription assay if a sufficient number of binding sites were probed at appropriate drug loadings.

In the present study we show that a wide range of time constants are observed in the transcription assay for the dissociation of actinomycin D from preferred binding sites. We also examine the effect of neighboring sequences on these dissociation kinetics. The ultimate objective was to elucidate general features of drug–DNA dissociation processes and to assess which of these may be amenable to modification as a possible means of modulating the dissociation process and thereby enhancing anticancer activity of such drugs. Several of these features have been identified and are discussed with respect to implications for possible drug design programs.

Actinomycin D was used as a model drug since it exhibited a variety of desired characteristics, including known time constants amenable to sampling times in the transcription assay (Phillips & Crothers, 1986), well-characterized sequence

† This work was supported by a grant from the Australian Research Grants Scheme.

0006-2960/88/0427-9122$01.50/0

specificity (Aivasashvilli & Beabealashvilli, 1983), and known detergent sequestering characteristics under transcription buffer conditions (Phillips & Crothers, 1986).

Materials and Methods

Materials. Actinomycin D (AMD)[1] was purchased from Calbiochem, and concentrations were determined spectrophotometrically by using an extinction coefficient of 24 450 M^{-1} cm^{-1} at 440 nm (Bittman & Blau, 1975). *Escherichia coli* RNA polymerase (*E. coli* RNAP) was purchased from New England Biolabs. Ultrapure ribonucleotides, 3′-*O*-methylnucleoside triphosphates, deoxynucleotides, GpA [guanylyl(3′→5′)adenosine], ribonuclease inhibitor (human placenta), BSA (RNase/DNase free), and the vector pPL λ were obtained from Pharmacia. [α-^{32}P]UTP (3000 Ci/mmol and 10 mCi/mL) and X-ray film (Hyperfilm-βmax) were obtained from Amersham. Heparin and SDS (molecular biology reagent) were purchased from Sigma. Urea, agarose, bis(acrylamide), acrylamide, ammonium persulfate, and TEMED were obtained from Bio-Rad as electrophoresis purity reagents. Restriction endonucleases and DNA polymerase I (Klenow fragment) were from Boehringer-Mannheim. NA45 DEAE membrane filters were obtained from Schleicher and Schuell. T4 DNA ligase was obtained from Bresa, Australia. Calf thymus DNA was obtained from Calbiochem, and the nucleotide concentration was quantified by using E_{260} = 6600 M^{-1} cm^{-1}. All other chemicals were of analytical reagent grade, and all solutions were prepared by using distilled, deionized, and filtered water from a Milli-Q four-stage water purification system (Millipore).

DNA Source. A 203-bp *Eco*RI restriction fragment of *lac* DNA containing the L8-UV5 double mutant was supplied by Professor D. M. Crothers (Yale University). The 203 fragment was ligated into the unique *Eco*RI site of pBR322 and the desired orientation selected by restriction enzyme analysis. Removal of potentially interfering Tet and P1 promoters was enabled by excising a *Bam*HI, *Hin*dIII fragment and filling in the 5′ overhanging ends with Klenow fragment and then ligating the blunt ends. Modifications made to the plasmid were confirmed by RNA sequence analysis.

The construction of an alternative vector involved the use of the inducible expression vector pPLλ that contained the strong leftward promoter of bacteriophage λ. To insert the UV5-containing fragment into the plasmid, the 5′ overhanging ends of the 203 fragment were filled in with Klenow fragment, and the blunt end fragment was then ligated into the unique *Hpa*I site of pPLλ. Screening for the presence of the UV5 fragment and selection for the desired orientation were achieved by restriction enzyme analysis and confirmed by RNA sequencing.

The recombinant pBR322 plasmid was transformed into *E. coli* HB101, while the recombinant pPLλ plasmid was transformed into *E. coli* N99cI$^+$, both by using the calcium chloride/rubidium chloride procedure of Hanahan (1983). The *lac* UV5 containing plasmids were amplified with 170 μg/mL chloramphenicol and isolated by using a modification of the alkaline lysis procedure of Maniatis et al. (1982). The isolated pBR322-UV5 plasmid was digested with *Pvu*II and *Sal*I, and a 497-bp fragment containing the UV5 promoter was isolated by electrophoresis through a 1.5% agarose gel in TBE buffer. The DNA fragment containing the UV5 and λP_L promoters (denoted UV5-λP_L) was isolated from the recombinant plasmid by using *Bam*HI and yielded a 1343-bp fragment. The fragments were electrophoresed onto NA45-DEAE paper and eluted into a buffer containing 20 mM Tris-HCl (pH 8.0), 2 mM EDTA, and 1.5 M NaCl by heating at 65 °C for 2 h and then phenol extracted, ethanol precipitated, and finally taken up in buffer containing 10 mM Tris-HCl (pH 8.0) and 1 mM EDTA. Concentration and integrity of the DNA were determined by ethidium bromide titration by comparison to a plasmid standard determined spectrophotometrically with E_{260} = 6600 M^{-1} cm^{-1}.

The relevant DNA sequences of the two promoter-containing fragments are

```
L8-UV5:   GAATTGTGAGCGGATAACAATTTCACACAGGAAACAGCTATGACCATGATTACGGATTCACTGG
          AATTCTCATGTTTGACAGCTTATCATCGATAAGCTGATCCTCTACGCCGGACGCATCGTGGCCG

UV5-λP_L: GAATTGTGAGCGGATAACAATTTCACACAGGAAACAGCTATGACCATGATTACGGATTCACTGG
          ATATAACTGGTTTTGCGCTTACCCCAACCAACAGGGGATTTGCTGCTTTCCATTGAGCCTGTTT
```

where the first two nucleotides result from initiation with GpA and correspond to the −1 and +1 position of the promoter.

In Vitro Transcription. Transcription conditions employed were a modification of those used by Phillips and Crothers (1986). The transcription buffer (Tc buffer) used contained 40 mM Tris-HCl (pH 8.0), 100 mM KCl, 3 mM $MgCl_2$, 0.1 mM EDTA, 5 mM DTT, 0.5 mg/mL BSA, and 1 unit/μL RNase inhibitor.

A binary complex was formed by incubating the 497- or 1343-bp fragment (50 nM) with *E. coli* RNAP (100 nM) for 15 min at 37 °C in Tc buffer. To remove any nonspecifically bound RNAP and to ensure a single round of transcription, heparin (in Tc buffer) was added to a final concentration of 400 μg/mL and the mixture incubated at 37 °C for 5 min. A stable initiated ternary complex was then formed by the addition of a nucleotide mix containing GpA (to 200 μM), UTP, GTP, ATP (to 5 μM) and [α-^{32}P]UTP in Tc buffer and incubated for 5 min at 37 °C. This procedure resulted in a high yield of ternary complex with a nascent RNA of mainly 10 nucleotides, due to initiation exclusively at the −1 position by the dinucleotide. The initiated complex was then divided into two aliquots; to one aliquot was added actinomycin D (to give a final concentration of 4 μM) in Tc buffer and to the other, an equal volume of Tc buffer. Following incubation at 37 °C for 30 min (Aivasashvilli & Beabealashvilli, 1983) an elongation nucleotide mix was added to both aliquots to give simultaneous elongation of transcription. The elongation mix gave a final concentration of all nucleotides of 2.5 mM and increased the final KCl concentration to 400 mM. High levels of KCl and nucleotides are thought to minimize pausing by increasing the elongation rate of the enzyme (Neff & Chamberlin, 1980). The high levels of nucleotides during elongation also diluted the radioactive nucleotide to the extent that subsequent incorporation was negligible. Incubation was continued at 37 °C, and aliquots were then removed at a range of time intervals for both added drug and elongation and transcription stopped by the addition of an equal volume of loading terminating buffer (10 M urea, 10% sucrose, 40 mM EDTA, 0.1% xylene cyanol, 0.1% bromophenol blue in 2 × TBE, pH 8.3) and placed on ice.

Sequencing of RNA Transcripts. Sequencing of the RNA was based on a modification of the method used by Reisbig and Hearst (1981) involving the use of 3′-*O*-methyl-CTP and 3′-*O*-methyl-ATP. To obtain sequence information from the initiated to the full-length transcript, a portion of the initiated complex was divided into two parts, and to one an elongation

[1] Abbreviations: AMD, actinomycin D; BSA, bovine serum albumin; SDS sodium dodecyl sulfate; Tris, tris(hydroxymethyl)aminomethane; EDTA; ethylenediaminetetraacetic acid; DTT, dithiothreitol; RNase, ribonuclease; RNAP, RNA polymerase; Tc, transcription; UTP, uridine 5′-triphosphate; GTP, guanosine 5′-triphosphate; ATP, adenosine 5′-triphosphate; CTP, cytosine 5′-triphosphate; TBE, Tris–borate–EDTA; bp, base pair.

nucleotide mix was added that contained a final concentration of 90 μM of the 3′-*O*-methyl-modified nucleotide and 10 μM of normal substrate. To obtain sequence information over the first 100 nucleotides, the sequencing reaction was generally allowed to proceed for 5 min at 37 °C, while sequence information for the full-length transcript was obtained by elongation for approximately 15 min at 37 °C. Sequence reactions were stopped by addition of a equal volume of loading terminating buffer. The positions of drug-induced pauses were determined by comparison with sequencing lanes run on the same gel.

Gel Electrophoresis of RNA Transcripts. Following exposure of the initiated complex to drug, elongation, and sequencing reactions, samples were placed at 90 °C for 5 min and then placed on ice. Samples were directly loaded on a 0.35 mm × 40 cm 12% denaturing gel [19:1 acrylamide/bis(acrylamide)] in TBE buffer. Gels were preelectrophoresed for 2–3 h at 2000 V and 95 W to bring the temperature of the gel to 55–60 °C, thus ensuring denaturing conditions. Electrophoresis was continued until the bromophenol blue had migrated off the bottom of the gel.

Following electrophoresis, gels were fixed in 10% acetic acid/10% methanol for 20 min and then dried under vacuum for 20 min. Fixing and drying of the gels were found to be necessary to improve resolution of the autoradiograms as well as to remove contaminants found in the commercial preparations of [α-^{32}P]UTP that would otherwise cloud the bottom third of the autoradiogram (equivalent to the first 30 bases on the gel). Autoradiography using Amersham Hyperfilm-βmax or Kodak XAR-5 X-ray film without intensifying screens usually required overnight exposure at room temperature.

Quantitation of RNA Transcripts. Autoradiograms were scanned by using a Biomed Model SL-504-XL laser densitometer linked to a Spectra Physics SP4270 integrator. Each lane was normalized with respect to the total amount of radioactivity, and actinomycin D induced pauses were calculated as a percentage of this total radioactivity.

RNA Hairpin Helices. The possible formation of RNA hairpin helices was analyzed by using the program HAIRGU, a modification of HAIRPN (Staden, 1978), constraining the loop to 3–25 nucleotides and the helix region to a minimum of 4 bp. Thermodynamic stability of each possible hairpin helix was quantitated by using the free energy values and procedure of Tinoco et al. (1973).

RESULTS

Drug-Induced Pausing. Figure 1 shows the effect on transcription by *E. coli* RNAP in the presence and absence of AMD. In each case the transcription was synchronized by elongation from a initiated complex due to the omission of CTP. The omission of CTP should have restricted RNA synthesis to 10 bases; however, minor read-through occurs to produce a 17-mer and a smaller quantity of a 23-mer. This read-through is presumably due to either misincorporation of other nucleotides in place of CTP or trace levels of contaminating CTP and has been previously noted by Carpousis and Gralla (1985) using the UV5 promoter and by Levin et al. (1987) with the T7 A1 promoter.

Elongation in the absence of drug (Figure 1) clearly shows production of a 380-base full-length transcript in less than 1 min with no further transcription subsequent to this. This, together with the time-dependent development of the sequencing lanes, provides direct evidence for the synchronous elongation of all active ternary complexes following the addition of CTP. Complete elongation is expected in this time on the basis of maximal rates of 20–30 nucleotides/s (von Hippel et al., 1984) under the optimal conditions employed. The conditions of high concentrations of heparin, KCl, and all four ribonucleotides were found to minimize natural pausing (data not shown) previously observed by Maizels (1973) from the UV5 promoter.

Table I: Characteristics of Drug-Induced Block Sites[a]

site no.	transcript length	drug site sequence	*A*	10^3k (s^{-1})
1 (fast)	37	ACAGCTAT	17.0	37.0
1 (slow)			2.3	0.34
2	43	ATGACCAT	3.4	9.6
3	82	ACAGCTTA	6.7	1.0
4	97	TAAGCTGA	6.7	3.5
5	117	GACGCATC	11.0	0.8
6	149	GGTGCGGT	9.0	1.2
pause	53	TACGG		
pause	112	GCCGG		

[a] The RNA length associated with the six drug-induced block sites is shown together with the DNA sequence at that site. The location of major blocked transcript is underlined in each case. The relative amplitude (*A*) and dissociation rate constant (*k*) is shown for read-through of RNA past each drug site. Amplitudes were not corrected for the statistical probability that some drug sites lie behind occupied upstream sites.

Incubation of 4 μM AMD with the initiated complex (30 min at 37 °C) results in a radical change in the elongation of the *E. coli* RNAP with sequence-dependent drug-induced pauses clearly being evident (Figure 1). At such pauses it is also evident that there is a sequence-dependent occupancy and release from that pause. The sequence associated with the first six of the drug-induced pauses is shown in Table I. In each case the polymerase reads through up to the center of apparent intercalation site. The consensus sequence[2] associated with five of the six sites is GpC; the sixth and much weaker site is ApC.

All of the preformed initiated complexes elongated efficiently in the presence of AMD, consistent with the observation by Straney and Crothers (1987) that AMD does not destabilize the initiated complex but in conflict with the notion of Sobell (1985) that AMD may have a direct effect on the stability of ternary complexes.

Quantitation of Multisite Drug Kinetics. To quantitate individual transcripts corresponding to drug inhibition sites, each lane was scanned with a densitometer and each band of a lane then normalized with respect to the total radioactivity in that lane. No allowance was made for further incorporation of [α-^{32}P]UTP past the production of the initiated complex, as the high levels of UTP (i.e., 2.5 mM) at elongation diluted the label to the point that further incorporation was negligible.

For each AMD site the individual transcripts resulting from drug-induced blockage were summed and expressed as a percentage of total radioactivity. The plot shown in Figure 2 therefore gives the normalized RNA mole fractions (as a percent) for each AMD site, as well as for the full-length transcript, at various times after elongation of the initiated complex. A small amount of full-length transcript is apparent at zero time and reflects the rapid production of full-length transcript (of the order of 10 s) from a small proportion of templates that do not have AMD bound in the transcribed region. Figure 3 represents a first-order kinetic analysis for the six AMD sites observed. In agreement with the work of Phillips and Crothers (1986), all sites exhibited a first-order process expected on the assumption that the progression of RNA polymerase past each drug site ("read-through") depends

[2] All sequences shown employ the 5′–3′ notation.

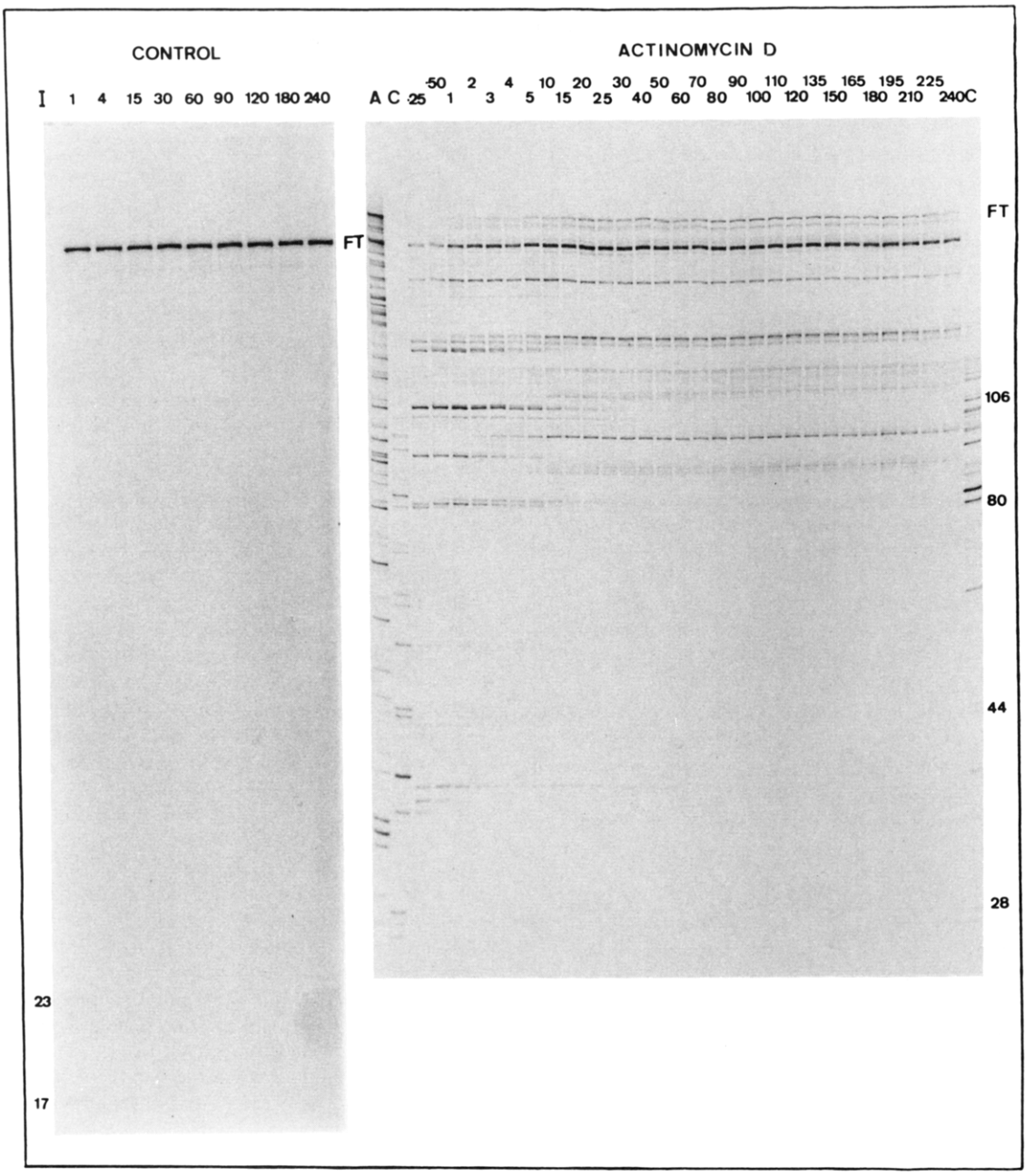

FIGURE 1: Multiple actinomycin D block sites (497 bp, UV5 fragment). The autoradiogram shows RNA lengths at time intervals (0.25–240 min) after the elongation phase was commenced by the addition of CTP, both in the absence (control lanes) and in the presence of actinomycin D. The initiated complex is shown in lane I (where some read-through is apparent from the first C of the initiated complexes to the second (17-mer) and third C (23-mer). The A and C lanes are sequencing lanes where the initiated complex was elongated in the presence of 3′-methoxy-ATP and 3′-methoxy-CTP, respectively. The full-length transcript is denoted as FT.

on the dissociation of drug from the DNA.

For the determination of kinetic parameters at the AMD binding sites, the concentrations of RNA of defined lengths ($[RNA]_i$, where i is the sequential block site number) corresponding to drug-induced inhibition were defined as

$$[RNA]_1 = A_{1f}e^{-k_{1f}t} + A_{1s}e^{-k_{1s}t}$$

$$[RNA]_2 = A_2e^{-k_2t} + (A_2/100)[RNA]_1$$

$$[RNA]_3 = A_3e^{-k_3t} + (A_3/100)[RNA]_1 + (A_3/100)[RNA]_2 + (A_3/100)[RNA]_{P53}$$

$$[RNA]_4 = A_4e^{-k_4t}$$

$$[RNA]_5 = A_5e^{-k_5t} + (A_5/100)[RNA]_{P112}$$

$$[RNA]_6 = A_6e^{-k_6t} + (A_6/100)[RNA]_{P112} + (A_6/100)[RNA]_5$$

The amplitude (A_i) represents the percentage of all RNA molecules corresponding to that particular length. For the first drug site, the rate of RNA elongation is described by two kinetically distinguishable processes (see Figure 3), and the fast and slow components are presented by f and s, respectively. The equations define a first-order rate of decay of the RNA concentration at each drug-induced pause, and additional terms allow for read-through from preceding sites where applicable. The read-through is experienced at downstream sites only if those sites are occupied by drug on individual DNA molecules, and this is reflected by a fractional occupancy term (i.e., fractional amplitude) in the equations.

There is no read-through of RNA polymerase past drug sites 3 and 4 (Figure 4). This greatly simplifies the kinetic analysis, and the equation for the site immediately downstream is reduced to a first-order decay. Release of RNA from two natural pauses of 53 and 112 bases (designated P53 and P112,

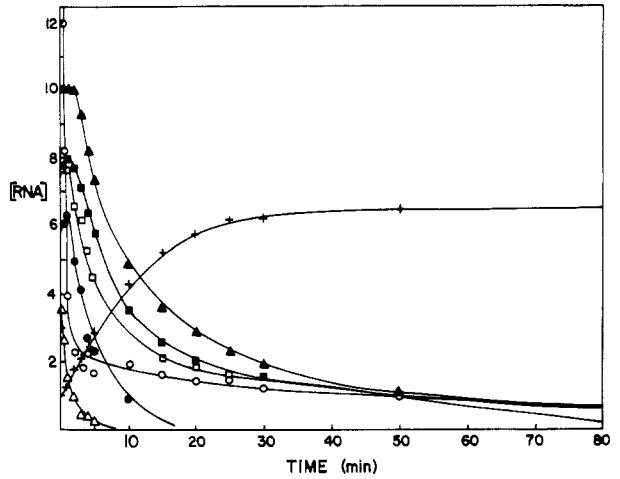

FIGURE 2: Kinetic profiles of transcripts. The kinetics of elongation of RNA (Figure 1) is shown as the percentage of RNA in each lane, as a function of elongation time after the addition of CTP. Drug block sites were at 35–37 (site 1, ○), 42 and 43 (site 2, △), 80–82 (site 3, □), 96 and 97 (site 4, ●), 116 and 117 (site 5, ▲), and 147–149 (site 6, ■). The full-length transcript is also shown (+).

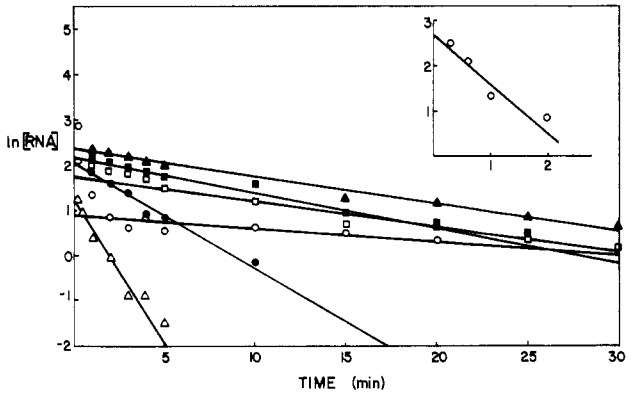

FIGURE 3: First-order kinetics at block sites. A first-order kinetic analysis of the relative RNA concentration (Figure 2) is shown for drug sites 1 (○), 2 (△), 3 (□), 4 (●), 5 (▲), and 6 (■). The inset shows a similar plot for early time points for elongation of transcription past drug site 1.

respectively) has also been considered in the above equations, so RNA released from these pauses contributes to the read-through to the drug site immediately downstream. For all drug sites the total read-through from earlier pauses or sites was less than 15% of the RNA concentration at the downstream drug sites over the entire sampling times measured.

The kinetic parameters determined from the first-order plots (Figure 3) are presented in Table I, and the rate constants derived are within 20% of values calculated by using the above equations. Such a deviation is consistent with errors of 10–20% experienced for the evaluation of RNA concentrations from densitometry and integration, and a more rigorous simulation of the kinetic parameters was not justified. Table I also provides the DNA sequence associated with each AMD binding site as well as the two pauses taken into account in deriving the kinetic equations. The most significant feature evident in the first-order plots of Figure 3 and the values presented in Table I is that drug dissociation rates can vary by more than an order of magnitude with regard to their respective rate constants, despite having a common tetranucleotide binding site.

An additional unexpected feature of the analysis seen again in Figure 3 and Table I is that site 1 is described by two first-order processes, one being relatively fast and the second and major process being a very slow dissociating event. A

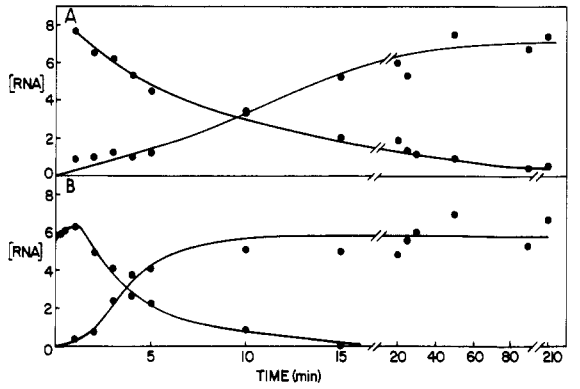

FIGURE 4: Termination of transcription. Drug-induced inhibition of transcription is shown for drug sites 3 (A) and 4 (B), together with the buildup of RNA some 10 bp downstream of each drug site.

change of drug loading from 4 to 2 and 1 μM AMD did not change the existence of these processes nor did elongation in the presence of 100 rather than 400 mM KCl (data not shown). However, when GTP was substituted for ITP in the elongation mix, a procedure that results in destabilization of RNA–RNA and RNA–DNA interactions (inosine forms less stable base pairs with cytidine than guanosine), the decay at site 1 (Figure 5) resorted to a single slow dissociating species. The slow dissociating species in the presence of ITP was characterized by the same slow rate constant seen when GTP was used. Under these conditions all other drug sites exhibited dissociation kinetics that were described by a single dissociation event.

Termination of Transcription. A striking feature of the AMD binding to the DNA template is the termination of transcription (Figures 1, 2, 4, and 6), and this is most clearly demonstrated by minimal full-length transcripts, even after several hours of elongation (Figure 1). This termination occurs in two ways: a defined halt to the progression of the RNAP at individual AMD binding sites, and an induced but broad halt downstream of particular AMD binding sites.

It is evident from Figure 1 that termination at the AMD binding site is dependent upon the length of the RNA at the site of drug inhibition. As the length of RNA increases, termination, as compared to read-through, increases so that AMD sites further downstream of the transcription initiation site produce a high degree of this mode of termination. This mode of termination was also noted with other intercalators and has also been observed by others (Flamée, 1985).

The second mode of termination of transcription by the induction of a broad halt downstream of the drug binding site is relatively unique to AMD and was not observed with nogalamycin and mithramycin, two DNA-binding drugs with similar dissociation kinetics. Echinomycin was the only other drug that exhibited similar termination, but it was less pronounced, with only some 10% termination observed at some sites (data not shown). This secondary mode of termination is seen at three of six sites analyzed and also occurred 7–10 nucleotides downstream of the AMD binding site. Sites 3 and 4 have associated termination that is 100% effective, in that all read-through from these two sites builds up at the termination sites downstream of the respective site (Figure 4). Site 5 also displays this induced termination but is only of the order of 50% effective and allowed some read-through from the termination region to sites downstream. When ITP was substituted for GTP in the elongation mix, the secondary, delayed termination was virtually eliminated (Figure 5).

Cooperative Drug Binding. The inhibition of transcription by AMD was also examined by using a UV5 promoter with

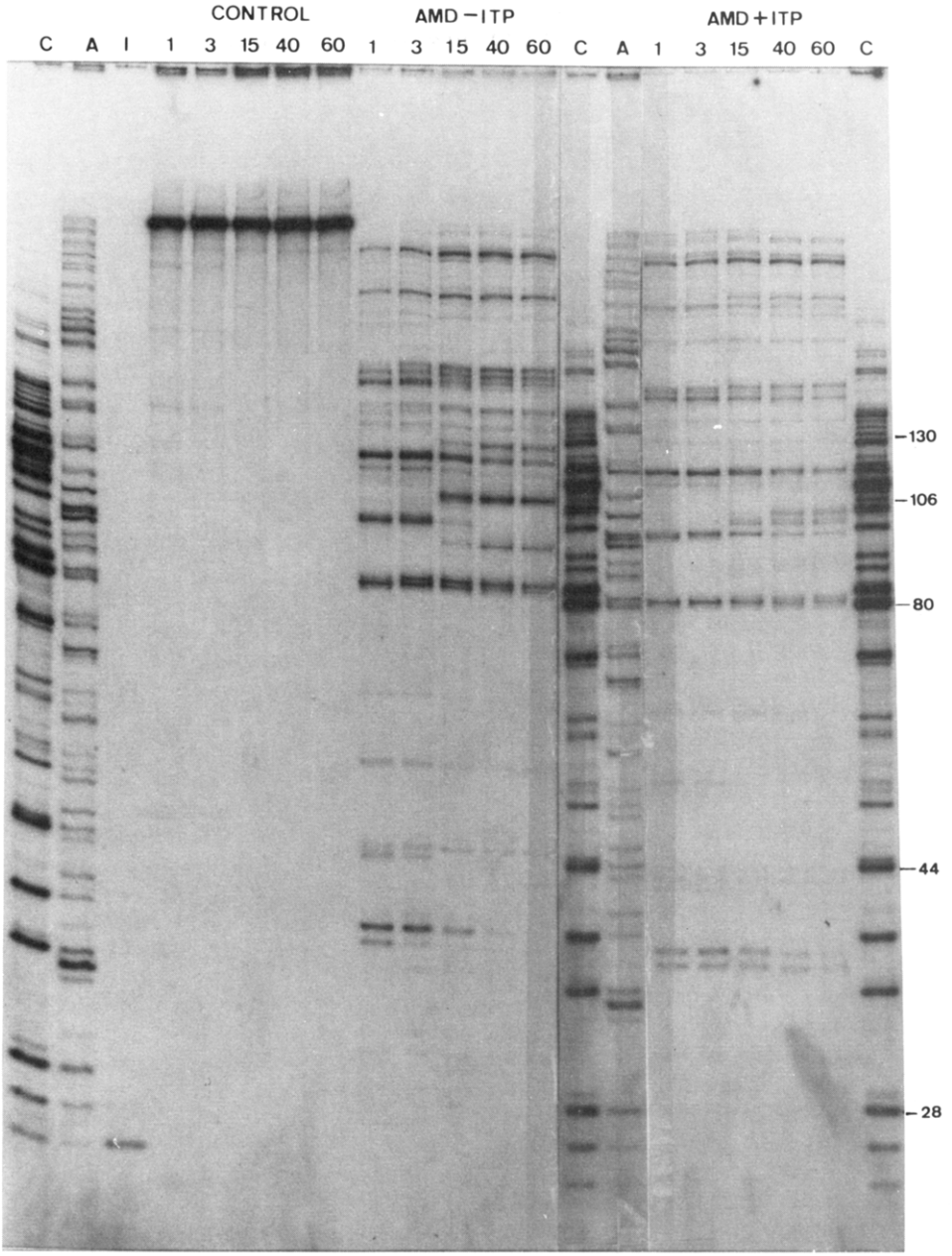

FIGURE 5: Effect of ITP on termination. The sequencing gel autoradiogram shows RNA lengths obtained 1–60 min after elongation of the initiated complex was begun by the addition of CTP. Control lanes are shown (absence of AMD), together with the effect of adding AMD to the initiated complex, both in the absence (AMD–ITP) and in the presence (AMD + ITP) of ITP. Sequencing lanes (C and A) reflect the addition of 3′-methoxy-CTP and 3′-methoxy-ATP, respectively, and lane I represents the initiated complex.

altered downstream region in which GC sites were close together (DNA fragment UV5-λP_L). The drug-induced block sites observed (Figure 6) were the same up to +67 as those seen when the UV5 497-bp fragment was used (with a common sequence up to +67). The block sites at 79 and 81 (TGCGCT) as well as 106 and 109 (TGCTGCT) exhibited significantly higher occupancy and much slower dissociation kinetics than the isolated high-affinity site at 37. These effects are unique only to adjacent GC binding sites and therefore demonstrate clear evidence of positive cooperativity. Termination of transcription is also associated with the drug sites at 79 and 87.

Discussion

Sequence Specificity of the Role of Flanking Sequences. This study has supported the well-documented GC specificity of AMD [for example, see Chen (1988), Dabrowiak (1983), Neidle and Abraham (1984), Robbie and Wilkins (1984), and Van Dyke et al. (1982)] in that all the high-affinity sites examined had GpC sequences at the intercalation site. This study has also strongly implicated sequences outside the binding tetranucleotide as being important determinants of sequence specificity. This effect is best illustrated at sites 1, 3, and 4, which all have the common AGCT tetranucleotide binding sequence but exhibit an order of magnitude difference in their occupancy and dissociation kinetics and hence selectivity for that site.

The tetranucleotide AGCT has been implicated by Van Dyke (1984) to be the most preferred of the AMD sites. The sequence specificity also fits into the model proposed by Aivasashvilli and Beabealashvilli (1983) of XGCY (X $\neq$ G, Y $\neq$ C) using an *E. coli* transcriptional system based on the T7 A1 promoter. The immediate effect of flanking sequences around the intercalation site, as shown by the above authors, is also observed in our studies. The significance of flanking A-T base pairs has also been reported recently (Chen, 1988).

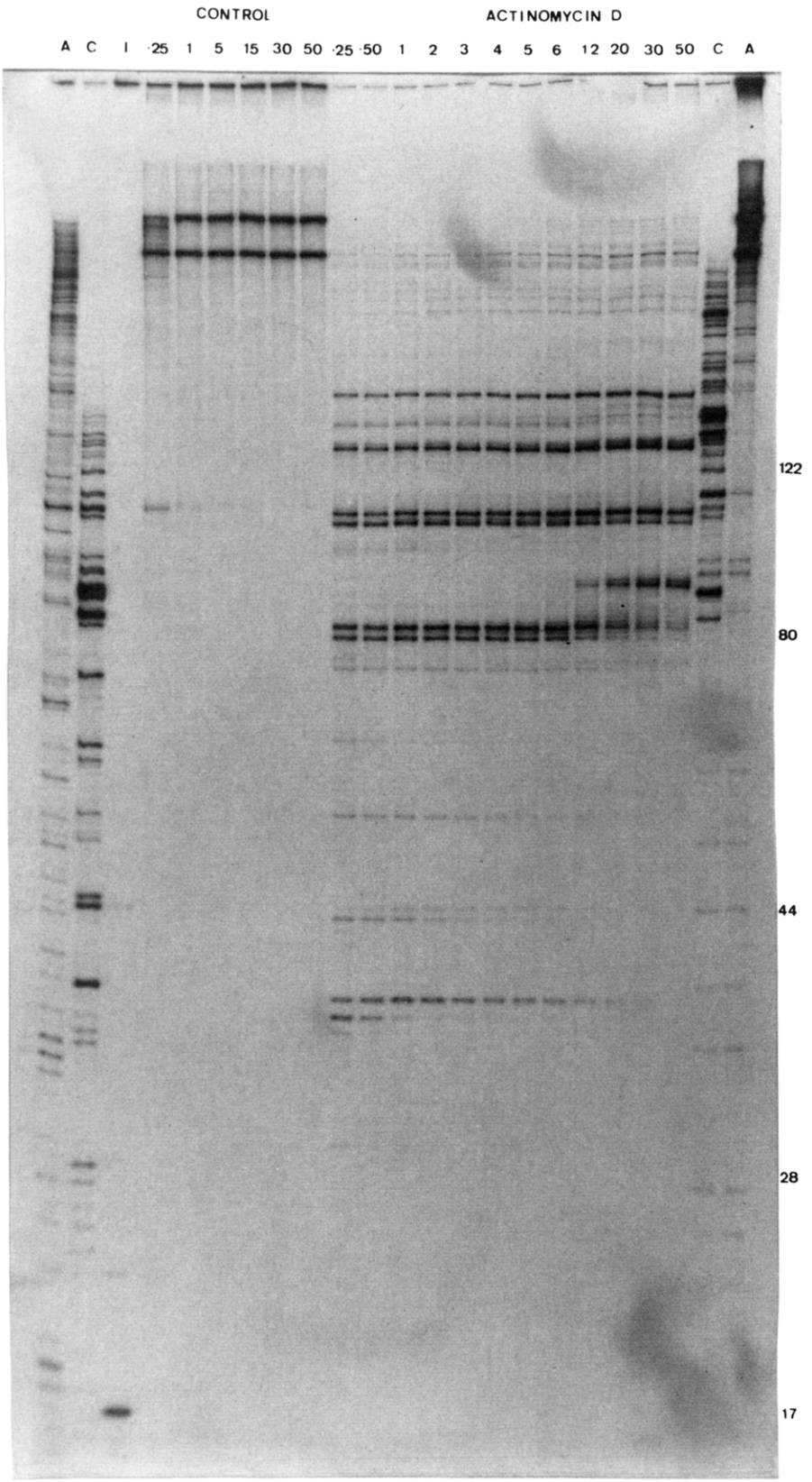

FIGURE 6: Multiple actinomycin D block sites (UV5-λP_L fragment). The autoradiogram shows RNA lengths at time intervals (0.5–50 min) after elongation commenced, in the absence and presence of AMD. The initiated complex (I) and sequencing lanes (A and C) are also shown. All lanes represent transcription from the UV5 promoter. The control lanes show a full-length transcript arising from the λP_L and UV5 promoters.

Sequences such as XGCC and GGCY seen in the UV5-λP_L fragment do not bind AMD, and in fact, as seen at site 2, ApC sequences bind AMD weakly in preference to such sequences but with relatively low occupancy and relatively fast dissociation kinetics. The observation that ApC sequences are seen as the second most favored dinucleotide is also consistent with the work of Van Dyke (1984) and is expected as the interaction at such dinucleotides suffers the loss of one hydrogen bond with the N2 amino group of guanine but no losses with respect to other interactions.

Transcription by *E. coli* RNAP from the UV5 promoter on an altered downstream DNA sequence (UV5-λP_L) has de-

tected a degree of cooperativity in the binding of AMD at sequences TGCGCT and TGCTGCT (Figure 6). Both these sequences have two AMD sites close together, and cooperativity was shown by high relative occupancies and slow dissociation kinetics at each site. This cooperative binding has also been observed by Scamrov and Beabealashvilli (1983) using DNase I footprinting. In contrast, extensive anticooperativity has been observed recently for adjacent GC sites (Scott et al., 1988). These studies serve to illustrate the subtle effect of transmitted distortions in the DNA structure by the AMD–DNA interaction (Pardi et al., 1983). Long-range effects have also been observed when AMD, intercalated into the G-C region of $d(C_{15}A_{15})\cdot d(T_{15}G_{15})$, resulted in transmission of perturbations to A-T pairs in the other half of the duplex (Early et al., 1977). Conversely, it is reasonable to expect that sequences removed from a potential binding site may equally exert a sequence-dependent influence on AMD binding. The data presented here do not allow conclusions to be drawn with regard to the influence of flanking sequences, as this would require an examination of multiple sites over a range of different sequences, and this is currently in progress.

An interesting aspect of the AMD-induced transcriptional blockage is that transcription can continue to the proposed "center" of the intercalation site, an aspect also noted in our laboratory for a variety of intercalating agents as well as for AMD inhibition of T7 RNA polymerase. For this to occur it would suggest that the leading edge of the melted region of the RNA–DNA hybrid, and hence the center of phosphodiester bond formation, coincides very closely to the boundary of the RNAP–DNA complex when in a stable ternary complex. A similar observation has been made by Shi et al. (1987) when investigating the effects of a psoralen adduct on the transcription by *E. coli* RNAP. These observations, together with the known location of AMD pentapeptides in the minor groove of DNA, suggest that the RNAP tracks along the major groove of DNA during active transcription. The use of DNA intercalating drugs in this assay has therefore provided a means of probing DNA–RNAP interactions.

Drug Occupancy. The relative drug occupancy at each site was obtained from the amplitude derived from the kinetic analysis presented in Figure 3. Preferred sites will exhibit a greater degree of occupancy than low-affinity sites, and this variation of occupancy will exist while the drug is in equilibrium with DNA prior to elongation. Consequently, the relative number of blocked polymerases at early elongation time intervals provides a direct reflection of the relative affinity at that site, so long as drug loading is adjusted to allow distribution over the whole template, resulting in only a small amount of full-length transcript.

The distribution of occupancies over the DNA template in this assay provides evidence for a realistic situation whereby all AMD sites do not have high levels of occupancy but rather there is sequence-dependent distribution over all available sites. This observation is particularly important considering the apparently high drug:bp ratio present in the transcription mix. The range of occupancies observed provides clear evidence that at the DNA level the available AMD is significantly less than calculated and significant losses occur, probably due to binding of AMD to the high concentration of protein present as part of the transcription buffer.

The recent observations of Brown and Shafer (1987) on the kinetics of association of AMD with mono-, oligo-, and polynucleotides showed little or no sequence or length dependence of AMD–DNA association kinetics. It is therefore reasonable to assume that a direct correlation should exist between the

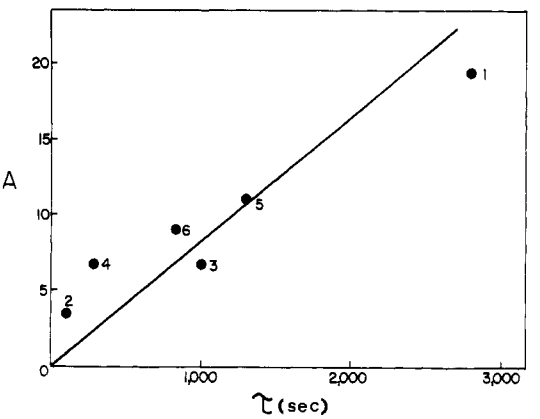

FIGURE 7: Amplitude of block sites and drug time constant. The relative amplitude associated with each AMD-induced block site (Figures 1 and 2; Table I) is shown as a function of the time constant for dissociation of AMD from each site.

time constant for dissociation and the relative occupancy of AMD at individual sites, and this has been confirmed (Figure 7). This correlation of AMD dissociation kinetics with occupancy at multiple sites on a heterogeneous DNA template enables the assessment of dissociation kinetics at individual sites to be carried out simply on the basis of relative occupancy at early time intervals of the elongation phase. This correlation has also been established by Forster et al. (1984), who found a linear relationship between DNA binding constants and the reciprocal of the dissociation rate constant for several anthracycline antibiotics.

Drug Dissociation Kinetics. The dissociation of intercalating drugs measured to date in "random-sequence" DNA gives rise to multiple dissociation exponentials due to site microheterogeneity (Krugh et al., 1980). The analysis of such data is in terms of a multiexponential fit, which represents an averaging of binding sites, within various resolvable kinetic processes (Phillips et al., 1988). The alternative approach is to examine the dissociation kinetics by using homopolymers such as poly(dG-dC), which yield single-exponential dissociation curves (Fox & Waring, 1984) but unfortunately fail to yield an unambiguous representation of drug action in vivo, where flanking sequences could have a major contribution to the drug–DNA interaction and have recently been documented (Chen, 1988). In addition to these factors, high levels of SDS are often used to induce dissociation of drug from the DNA, and the presence of the SDS raises questions as to the meaning of such data.

The method presented here provides a novel and biologically relevant means of obtaining the dissociation kinetics from a range of individual sites in heterogeneous DNA. The generalized view of AMD providing long-lived halts to the progress of the RNAP is substantiated by this assay, but with evidence that individual binding sites can vary by up to an order of magnitude with respect to their dissociation kinetics and hence their ability to inhibit RNAP. This variation is clearly seen at sites 1, 3, and 4 that, despite their common tetranucleotide binding site, show a 10-fold difference in dissociation kinetics. The inference again is that the flanking sequences and/or the conformational variations they are associated with are the cause of such variations, and this has been supported by recent NMR studies of Scott et al. (1988).

The relatively slow dissociation reactions seen with AMD have been proposed by Muller and Crothers (1968) to be due to conformational changes in the pentapeptide rings. More recently, NMR studies of Brown et al. (1984) and the computer modeling of Lybrand et al. (1986) have found little

change in pentapeptide conformations when AMD complexes with DNA, ruling out the possibility that extensive conformational changes take place in the drug upon binding. The large variation in the dissociation constants derived from this assay for GpC sites suggests that the DNA sequence itself and the various influences associated with flanking sequences are the most important determinants of AMD slow kinetics. This is in agreement with studies of Krugh et al. (1980), which indicated site heterogeneity in natural DNA that led to the multistep nature of the slow dissociation of the drug–DNA complex.

The observations of Hogan and Austin (1987) that the 434 repressor binding affinity can be reduced at least 50-fold in response to a sequence change at the center of the 434 operator suggest that it would also be reasonable to expect that sequence variations could have a profound effect on drug dissociation kinetics. To confidently determine the properties of the DNA that give rise to slow kinetics, a more extensive analysis would be required of a number of individual binding sites in heterogeneous DNA.

Termination of Transcription at the Drug Site. A consequence of the present in vitro AMD–DNA transcription studies has been the observation and quantitiation of a significant but unexpected phenomena, the termination of transcription. The studies of Flamêe (1985) reported that AMD, in certain instances, results in the termination of transcription of T7 DNA, but most often the antibiotic was released before RNAP detached from the template DNA. The present work has enabled some understanding of the mechanistic basis for these events.

Termination of transcription at individual drug sites is dependent to some extent on the length of the transcript at the drug site. This length dependence probably derives from the increased mechanical stress placed on the ternary complex as the length of the nascent RNA increases. The termination at the drug site is also dependent upon the rate of dissociation of the drug from the DNA—the slower the AMD dissociated from the DNA, the greater the proportion of the molecules that terminated, rather than paused, at that site. This effect was even more pronounced with nogalamycin (unpublished data). The influence of dissociation kinetics on the termination process can therefore be related simply to the time-dependent nature that the mechanical stresses have on the ternary transcriptional complex, and this has been alluded to previously (Straney & Crothers, 1987).

Delayed Drug-Induced Termination of Transcription. The use of ITP instead of GTP in the elongation mix resulted in virtually total loss of the broad band of drug-induced termination products (Figure 5). This suggests that the delayed termination phenomena are associated with RNA hairpin helices, which are less stable when ITP is incorporated into the RNA chain instead of GTP. The most likely model for this phenomenon is that inhibition of transcription at a drug site allows sufficient time for a stable hairpin helix to form in the previously transcribed RNA.

A general drug-dependent model of termination of transcription is shown in Figure 9 and is based on the models for rho-independent termination of Platt (1986). In these models, a stable hairpin helix and a 3′-terminal stretch of consecutive uridine residues in the transcript are required in order to facilitate termination. The hairpin helix alone is able to elicit pausing of RNAP, but efficiency of termination depends on a combination of the stability of the hairpin and instability of the rU·dA duplex (von Hippel et al., 1984; Platt, 1986). The drug-dependent termination model assumes that pausing at a drug site provides sufficient time for an RNA hairpin helix to form in the transcribed RNA. The extent of formation of the hairpin helix will vary depending on the size of the loop, number of bulges, thermodynamic stability, etc. and will result in a varying degree of efficiency of termination. After the

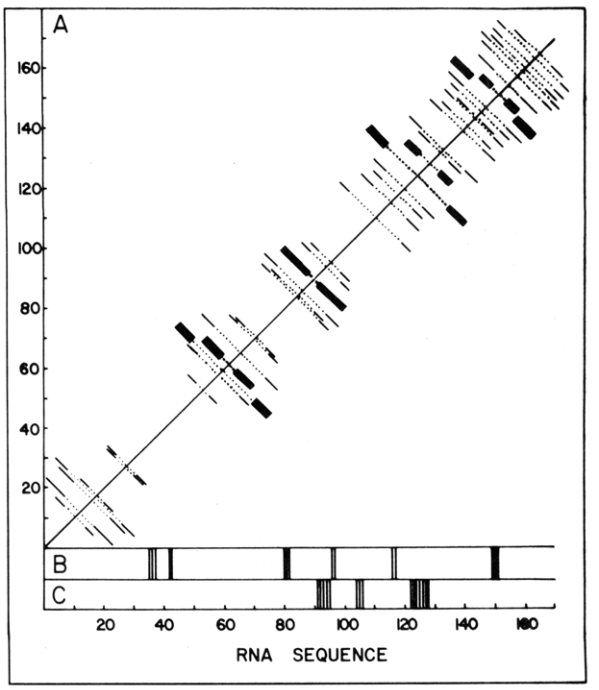

FIGURE 8: Hairpin helices in UV5 497-bp transcript. All possible RNA hairpin helices (at least 4 bp with 3–25 nucleotides in the loop) are shown (A) in a diagonal display where the numbering on both axes represents the RNA length from the −1 position. The four helical regions, calculated (Tinoco et al., 1973) to be thermodynamically stable (<−30 kJ/mol), three of which contain a bulge, are shown are thick continuous lines, while all other less stable helices are shown as a thin line interspersed with dots to represent the number of nucleotides in the hairpin loop. The location of AMD block sites is shown in (B), and termination regions are shown in (C).

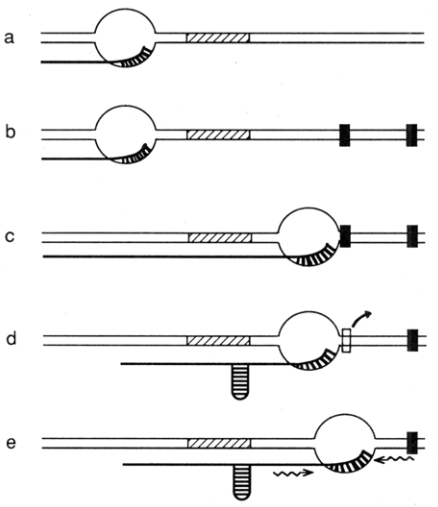

FIGURE 9: Model of AMD-induced termination of transcription. The stable initiated complex (a) is shown after addition of drug (b). Elongation up to a drug site is shown in (c). Pausing of the RNA polymerase at the drug site provides sufficient time for the formation of an RNA hairpin helix in the transcribed RNA (d) prior to dissociation of the drug from that site. The region coding for the RNA hairpin helix is hatched and is approximately 15 bp upstream of the drug binding site. After dissociation of the drug from the DNA, elongation proceeds past the drug site until termination is induced by a combination of destabilizing effects from the RNA hairpin helix and from transmitted conformational effects from downstream drug sites (e).

RNA hairpin helix has formed and drug dissociated from that site, elongation continues until termination occurs as a result of the cumulative destabilizing effect of the RNA hairpin helix and conformational effects from downstream drug sites (Figure 9). This model therefore suggests two major features to account for a drug-dependent termination process—the drug must have a long residence time on the DNA, and it must also exhibit long-range conformational effects along the DNA. The model also predicts that the number of nucleotides transcribed after the drug site will vary, depending on the location of the next downstream drug site, and this variation is indeed observed (Figure 6).

The termination model (Figure 9) assumes an energetically favorable RNA hairpin helix, the 3′ end of which is approximately 15 nucleotides upstream of the drug binding site. The RNA up to 15 nucleotides of the drug inhibition site is therefore the critical hairpin-forming region and is outside the RNA domain known to be intimately associated with DNA in the transcription ternary complex. It also allows for a few nucleotides between the RNA hairpin and RNA in the transcription complex. Drug sites 3–5 are consistent with such a drug-induced termination model. For site 3, complete formation of the RNA hairpin helix is probably achieved after dissociation of AMD from that site. No thermodynamically stable helices exist in the RNA sequence prior to drug sites 1 and 2 (Figure 8).

Biological Implications. The detection of drug-induced termination of transcription is of immense potential significance to understanding of the mode of action of DNA-binding drugs. The classical picture of drug-induced inhibition of transcription now appears too simplistic and may need to be revised to accommodate this termination phenomenon.

It the mode of action of some DNA binding anticancer drugs was due in part to drug-induced termination of transcription, then this mechanism offers a new means of enhancing drug cytotoxicity. It will be necessary to establish if the proposed RNA hairpin helix model adequately accounts for this effect and to elucidate those features of the drug that contribute to the termination phenomenon. Once these features have been adequately defined, it may then be possible to append these features to existing, clinically useful anticancer drugs, with the prospect of enhancing drug activity and therefore enabling lower drug levels to be employed with a corresponding decrease of the well-known side effects of these cytotoxic agents.

ACKNOWLEDGMENTS

We thank Professor Don Crothers for the 203-bp *lac* UV5 fragment and Halina Trist for assistance with isolation of plasmids and promoter fragments.

Registry No. AMD, 50-76-0.

REFERENCES

Aivasashvilli, V. A., & Beabealashvilli, R. Sh. (1983) *FEBS Lett. 160*, 124–128.

Aktipis, S., & Panayotatos, N. (1981) *Biochim. Biophys. Acta 655*, 278–290.

Bernasconi, C. F. (1976) *Relaxation Kinetics*, Academic, New York.

Bittman, R., & Blau, L. (1975) *Biochemistry 14*, 2138–2145.

Brown, J. R. (1978) *Prog. Med. Chem. 15*, 125–164.

Brown, S. C., & Shafer, R. H. (1987) *Biochemistry 26*, 277–282.

Brown, S. C., Mullis, K., Leenson, C., & Shafer, R. H. (1984) *Biochemistry 23*, 403–408.

Carpousis, A. J., & Gralla, J. D. (1985) *J. Mol. Biol. 183*, 165–177.

Chaires, J. B., Dattagupta, N., & Crothers, D. M. (1985) *Biochemistry 24*, 260–267.

Chen, F. (1988) *Biochemistry 27*, 1843–1848.

Dabrowiak, J. C. (1983) *Life Sci. 32*, 2915–2931.

Denny, W. A., Atwell, G. J., Baguley, B. C., & Wakelin, L. P. G. (1985) *J. Med. Chem. 28*, 1568–1574.

Early, T. A., Kearns, D. R., Burd, J. F., Larson, J. E., & Wells, R. D. (1977) *Biochemistry 16*, 541–551.

Feigon, J., Denny, W. A., Leupin, W., & Kearns, D. R. (1984) *J. Med. Chem. 27*, 450–465.

Flamée, P-A. (1985) *Biochim. J. 230*, 557–560.

Forster, W., Stutter, E., & Salyanov, V. I. (1984) *Stud. Biophys. 104*, 45–56.

Fox, K. R., & Waring, M. J. (1981) *Biochim. Biophys. Acta 654*, 279–286.

Fox, K. R., & Waring, M. J. (1984) *Eur. J. Biochem. 145*, 579–586.

Gabbay, E. J., Grier, D., Fingerle, R. E., Reimer, R., Levy, R., Pearce, S. W., & Wilson, W. D. (1976) *Biochemistry 15*, 2062–2070.

Gandecha, B. M., Brown, J. R., & Crampton, M. R. (1985) *Biochem. Pharmacol. 34*, 733–736.

Hanahan, D. (1983) *J. Mol. Biol. 166*, 557–580.

Hogan, M. E., & Austin, R. H. (1987) *Nature (London) 329*, 263–266.

Krugh, T. R., Hook, R. J., & Balakrishnan, M. S. (1980) in *Nucleic Acid Geometry and Dynamics* (Sarma, R. H., Ed.) pp 351–366, Permagon, New York.

Levin, J. R., Krummel, B., & Chamberlin, M. J. (1987) *J. Mol. Biol. 196*, 85–100.

Lybrand, T. P., Brown, S. C., Creighton, S., Shafer, R. H., & Kollman, P. A. (1986) *J. Mol. Biol. 191*, 495–507.

Maizels, N. (1973) *Proc. Natl. Acad. Sci. U.S.A. 70*, 3585–3589.

Maniatis, T., Fritsch, E. F., & Sambrook, J. (1982) *Molecular Cloning—A Laboratory Manual*, Cold Spring Harbor Laboratory, Cold Spring Harbor, NY.

Muller, W., & Crothers, D. M. (1968) *J. Mol. Biol. 35*, 251–290.

Neff, N. F., & Chamberlin, M. J. (1980) *Biochemistry 19*, 3005–3015.

Neidle, S., & Waring, M. J., Eds. (1983) *Molecular Aspects of Anticancer Drug Action*, Macmillan, London.

Neidle, S., & Abraham, Z. (1984) *CRC Crit. Rev. Biochem. 17*, 73–121.

Pardi, A., Morden, K. M., Patel, D. J., & Tinoco, I. (1983) *Biochemistry 22*, 1107–1113.

Phillips, D. R., & Crothers, D. M. (1986) *Biochemistry 25*, 7355–7362.

Phillips, D. R., Greif, P. C., & Boston, R. C. (1988) *Mol. Pharmacol. 33*, 225–230.

Platt, T. (1986) *Annu. Rev. Biochem. 55*, 339–372.

Ralph, R. K., Marshall, B., & Darkin, S. (1983) *Trends Biochem. Sci. (Pers. Ed.) 8*, 212–214.

Reisbig, R. R., & Hearst, J. E. (1981) *Biochemistry 20*, 1907–1918.

Robbie, M., & Wilkins, R. J. (1984) *Chem.-Biol. Interact. 49*, 189–207.

Scamrov, A. V., & Beabealashvilli, R. Sh. (1983) *FEBS Lett. 164*, 97–101.

Scott, E. V., Jones, R. L., Banville, D. L., Zon, G., Marzilli, L. G., & Wilson, W. D. (1988) *Biochemistry 27*, 915–923.

Shi, Y-B., Gamper, H., & Hearst, J. E. (1987) *Nucleic Acids Res. 15*, 6843-6854.
Siegfried, J. M., Sartorelli, A. C., & Tritton, T. R. (1983) *Cancer Biochem. Biophys. 6*, 137-142.
Sobell, H. M. (1985) *Proc. Natl. Acad. Sci. U.S.A. 82*, 5328-5331.
Staden, R. (1978) *Nucleic Acids Res. 5*, 1013-1015.
Straney, D. C., & Crothers, D. M. (1987) *Biochemistry 26*, 1987-1995.
Tinoco, I., Bover, P. N., Dengler, B., Levine, M. D., Uhlenback, O. C., Crothers, D. M., & Gralla, J. (1973) *Nature (London) New Biol. 246*, 40-41.
Valentini, L., Nicolella, V., Vannini, E., Menozzi, M., Penco, S., & Arcamone, F. (1985) *Farmaco, Ed. Sci. 40*, 376-390.
Van Dyke, M. W. (1984) Ph.D. Thesis, California Institute of Technology.
Van Dyke, M. W., Hertzberg, R. P., & Dervan, P. B. (1982) *Proc. Natl. Acad. Sci. U.S.A. 79*, 5470-5475.
von Hippel, P. H., Bear, D. G., Morgan, W. D., & McSwiggen, J. A. (1984) *Annu. Rev. Biochem. 53*, 389-446.
Wakelin, L. (1986) *Med. Res. Rev. 6*, 275-340.
Wakelin, L. P. G., & Waring, M. J. (1980) *J. Mol. Biol. 144*, 183-214.
Wakelin, L. P. G., Atwell, G. J., Rewcastle, G. W., & Denny, W. A. (1987) *J. Med. Chem. 30*, 855-861.
Waring, M. J., & Fox, K. R. (1983) in *Molecular Aspects of Anticancer Drug Action* (Neidle, S., & Waring, M. J., Eds.) pp 127-156, Macmillan, London.
Wilson, D. W., Grier, D., Reimer, R., Bauman, J. D., Preston, J. F., & Gabbay, E. J. (1976) *J. Med. Chem. 19*, 381-384.
Wilson, W. D., & Jones, R. L. (1981) *Adv. Pharmacol. Chemother. 18*, 177-222.

Affinity Labeling of the GDP/GTP Binding Site in *Thermus thermophilus* Elongation Factor Tu[†,‡]

Marcus E. Peter,[§] Brigitte Wittmann-Liebold,[∥] and Mathias Sprinzl*[,§]

Laboratorium für Biochemie, Universität Bayreuth, Postfach 10 12 51, D-8580 Bayreuth, FRG, and Max-Planck-Institut für molekulare Genetik, Ihnestrasse 8, D-1000 Berlin-Dahlem, FRG

Received May 10, 1988; Revised Manuscript Received July 20, 1988

ABSTRACT: Elongation factor Tu from *Thermus thermophilus* was treated successively with periodate-oxidized GDP or GTP and cyanoborohydride. Covalently modified cyanogen bromide or trypsin fragments of the protein were isolated, and the position of their modification was determined. Lysine residues 52 and 137 were heavily labeled, lysine-137 being considerably more reactive in the GTP form as compared to the GDP form of the protein. These residues are in the proximity of the GDP/GTP binding site. Lys-325 was also labeled, but to a lower extent. The part of the EF-Tu containing residue 52 is missing in crystallized EF-Tu·GDP from *Escherichia coli* [Jurnak, F. (1985) *Science (Washington, D.C.) 230*, 32-36]. These results place the part of *T. thermophilus* EF-Tu corresponding to the missing fragment in *E. coli* EF-Tu in the vicinity of the nucleotide binding site and allow its role in the interaction with aminoacyl-tRNA and elongation factor Ts to be evaluated. Cross-linking of EF-Tu·GDP by irradiation at 257 nm showed that a sequence of 10 amino acids residues which is found in the *Thermus thermophilus* elongation factor Tu but not in other homologous bacterial proteins is located in the vicinity of the GDP/GTP binding site.

Elongation factor Tu (EF-Tu)[1] is a guanosine nucleotide binding protein which acts as a mediator of a new protein elongation cycle during protein biosynthesis (Miller & Weissbach, 1977). It interacts with GDP, GTP, elongation factor Ts, aminoacyl-tRNA, and ribosomes. The functional cycle of EF-Tu resembles that of other GTP binding proteins including transducin, the G-proteins in hormone receptor systems, and the poorly understood c-H-ras oncogene protein p21 (Gilman, 1987; Stryer & Bourne, 1986). Sequences of all these GTP binding proteins contain conserved sequences and domains pointing to similarities in their tertiary structures (Halliday, 1984; Gilman, 1987; Stryer & Bourne, 1986). For this reason, the elongation factor Tu from *Escherichia coli*, a GTP binding protein with a partially solved tertiary structure (Jurnak, 1985; la Cour et al., 1985), has become a model for the study of structure–function relationships of GTP binding proteins. This approach has, however, several disadvantages: First, the elongation factor Tu from *E. coli* is an unstable protein. It is susceptible to rapid thermal denaturation and is sensitive toward proteolytic cleavage. Second, this protein cannot be prepared in nucleotide-free form without rapid loss of its activity (Ohta et al., 1977) which seriously hampers structural and biochemical investigation. Third, although the high-resolution three-dimensional structure has been solved for the G binding domain of *E. coli* EF-Tu (Jurnak, 1985; la Cour et al., 1985), this was achieved by using a partially degraded protein which lacked a fragment of 14 amino acids (Jurnak, 1985).

To circumvent some of these problems, we have investigated the elongation factor Tu from the extreme thermophilic bacterium *Thermus thermophilus* (Degryse et al., 1978). This GTP binding protein is considerably more stable than EF-Tu from *E. coli* (Nakamura et al., 1978; Arai et al., 1978) and can be prepared in nucleotide-free form. These features fa-

[†] This work was supported by the Deutsche Forschungsgemeinschaft (SFB 213/D5) and the Fonds der Chemischen Industrie.

[‡] Dedicated to Prof. Fritz Cramer on his 65th birthday.

* To whom correspondence should be addressed.
[§] Universität Bayreuth.
[∥] Max-Planck-Institut für molekulare Genetik.

[1] Abbreviations: EF-Tu and EF-Ts, elongation factors Tu and Ts, respectively; aa-tRNA, aminoacyl transfer RNA; HPLC, high-performance liquid chromatography; PTH, phenylthiohydantoin.

0006-2960/88/0427-9132$01.50/0